Effects of Soil Depth Spatial Variation on Runoff Simulation, Using the Limburg Soil Erosion Model (LISEM), a Case Study in Faucon Catchment, France

Pooyan RAHIMY

Faculty of Geo-Information Science and Earth Observation, University of Twente, Enschede, Netherlands

Abstract: Soil depth is an important parameter for models of surface runoff. Commonly used models require not only accurate estimates of the parameter but also its realistic spatial distribution. The objective of this study was to use terrain and environmental variables to map soil depth, comparing different spatial prediction methods by their effect on simulated runoff hydrographs. The study area is called Faucon, and it is located in the southeast of the French Alps. An additive linear model of "land cover class" and "overland flow distance to channel network" predicted the soil depth in the best way. Regression kriging (RK) used in this model gave better accuracy than ordinary kriging (OK). The soil depth maps, including conditional simulations, were exported to the hydrologic model of LISEM, where three synthetic rainfall scenarios were used. The hydrographs produced by RK and OK were significantly different only at rainfalls of low intensity or short duration.

Keywords: conditional simulation; Faucon; hydrograph; kriging; LISEM; soil depth

The surface runoff is a source of erosion, gullies and flash floods in mountainous areas (De Roo 1996a). All measures to reduce these hazards require accurate runoff simulation. Important factors to be taken into consideration for runoff modelling are: (1) environmental parameters, including land cover/land use, topography and geology (Grayson & Bloschl 2001; Herbst & Diekkrüger 2006b; Shafique *et al.* 2011); (2) rainfall spatial variability (Singh 1997; Goovaerts 2000); (3) infiltration capacity of soil. The latter mostly depends on storage capacity of soil which is the effect of soil depth, porosity and initial soil moisture (Kutilek *et al.* 1994). If the soil does not have a sufficient storage capacity because of being shallow and/or having the high initial moisture, most of the rain will contribute to runoff generation. In other words, as explained by Green-Ampt model (Green & Ampt 1911; Neitsch *et al.* 2002), the surface water infiltration rate is inversely proportional to cumulative infiltration, i.e. storage capacity (Jetten 2002). Therefore, the soil depth strongly affects water infiltration and accordingly runoff generation (Neitsch *et al.* 2002; Herbst & Diekkrüger 2006a). Since in mountainous areas there are a wide variety of soils with different depths, the runoff generation amount differs spatially. The knowledge of more realistic spatial variations of this soil property would result in better hydrologic simulations. This will require an intensive soil survey which is difficult and expensive. Hence, knowing how far general or very detailed spatial variations of soil depth may influence the hydrologic modelling will guide researchers to plan optimally for future studies on runoff and flash flood modelling.

The soil depth covaries spatially with soil type and environmental variables (Dietrich *et al.* 1995; Minasny & McBratney 1999; Kuriakose *et al.* 2009). In a conventional soil survey, inaccessible parts of a catchment would be mapped by environmental and terrain parameters as predictors (McKenzie & Ryan 1999; McBratney & Mendonça Santos 2003; Penížek & Borůvka 2006). Some studies stated that using environmental factors such as slope, land use and land cover as the predictors of soil hydrologic properties will result in accurate outputs (Odeh *et al.* 1995; Merz & Bárdossy 1998; Kuriakose *et al.* 2009). Florinsky & Eilers (2002) reported that the spatial distribution of topsoil moisture content has a significant relationship with the topographic indices including slope gradient, aspect, plan curvature, specific catchment area and stream power index. Kalivas *et al.* (2002) observed that the morphometric parameter of distance to river could acceptably predict the sand and clay content of soil. Other researches have demonstrated that morphometric variables such as elevation and distance to stream are very much promising to be used as the predictors for soil depth (Herbst *et al.* 2006a, b; Ziadat 2010; Shafique *et al.* 2011). Best-predictor maps of soil depth give the best prediction at each location, but as a whole they do not realistically represent the spatial variation. For this, kriging and conditional simulation of soil depth will result in better representation of spatial variations (Webster & Oliver 2007). Odeh *et al.* (1995) and Herbst *et al.* (2006a, b) concluded that regression kriging using the slope attributes as co-variables is the most appropriate method with the least prediction errors for the soil depth mapping. Penížek and Borůvka (2006) also reported a similar result with the difference that the slope acted better when used in Co-Kriging. Kuriakose *et al.* (2009) obtained the most accurate maps of the soil depth when they applied regression kriging and land cover/land use as predictors. They also reported that conditional simulation would give better realization of soil depth.

The objectives of this study were: (1) to assess the ability of environmental and morphometric variables to map soil depth; (2) to examine the effect of different soil depth spatial variations on runoff simulation using the hydrologic model of LISEM (Jetten 2002).

MATERIAL AND METHODS

Study area

The study area called Faucon (Figure 1), centred at 44°25'N and 6°40'E (Hosein 2010), has a stream which is a tributary of the Ubaye River. The area's land use/land cover mainly consists of farms, prairies and forests of broadleaved and coniferous trees (Hosein 2010). The catchment has experienced 14 flash floods in the last century (OMIV-EOST 2010).

Data acquisition

Most of the basic data required for runoff simulation in the LISEM model (Jetten 2002), had been acquired by the Mountain Risks project (Mountain Risks 2010). Other data including soil properties and some site descriptions were obtained during field observations and laboratory work (Table 1).

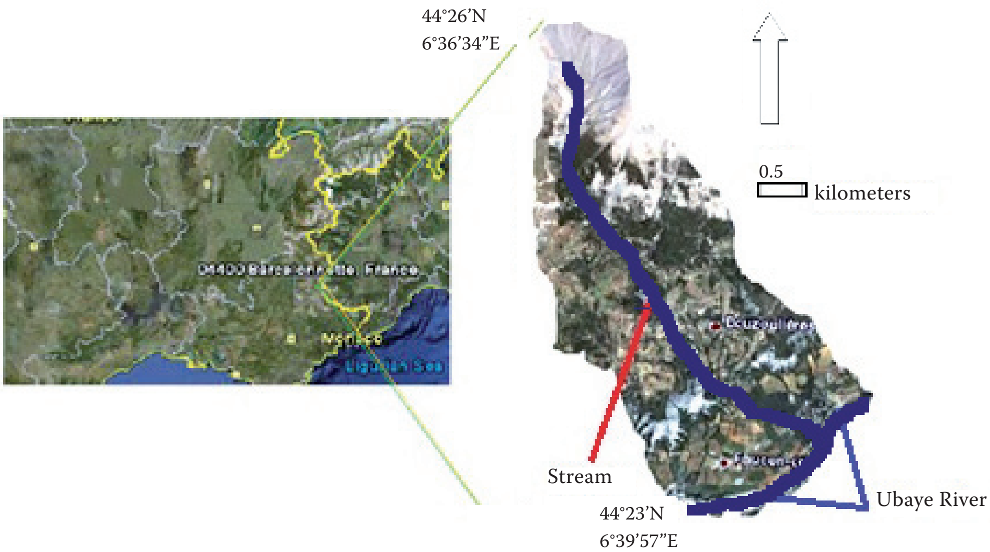

Figure 1. The Faucon hydrological sub-basin

Sample locations were determined by the stratified purposive sampling strategy for which the geomorphic and land cover maps were overlaid and on each resultant unit, at least one sampling point was selected, considering accessibility of the points (Figure 2). There were some available data on soil (Hosein 2010) sampled from the middle of the catchment which were also taken into consideration. In total, 64 sampling points were determined.

The soil depth was measured with an auger. Note that the soil depth was considered from the soil surface down to the bedrock, which includes all the soil horizons. The saturated hydraulic conductivity (*Ks*) was determined using the single-ring infiltrometer method (Bagarello & Sferlazza 2009; Farrel 2010). The surface stoniness and soil texture were determined using FAO and feel methods, respectively (FAO 2006; USDA 2010). Some other site observations, namely plant height and canopy cover at each land cover unit were recorded. The leaf area index (LAI) was then calculated by the WOFOST-Diepen equation (Jetten *et al.* 2010). Other soil parameters (Table 1) were measured in laboratory. The random roughness and Manning's coefficient parameters were also measured for each land cover unit, using the Manning and Random Roughness tables available in literature (Mwendera & Feyen 1992; Renard *et al.* 2000; Prachansri 2007). The measured parameters were then assigned to their corresponding units on the map shown in Figure 2. All the resulting maps were re-sampled to 15 m resolution by the nearest neighbour method. Since the LISEM assumes that the stream width is smaller than the cell size (Hessel 2005) and the maximum width of the Faucon stream was 9 meters, the cell size was set at 15 meters. Also, based on literature (Hessel 2005), because Chow's kinematic wave equation is used in the LISEM (Jetten 2002), selecting the grid size equal or less than 15 meters causes stability between *dt* (time component) and *dx* (distance component) of the differential kinematic wave equation and results in realistic outputs (Hessel 2005).

Hydrologic analysis of the catchment

The runoff ratio of the catchment was calculated by the following equation:

$$C = \sum_{i=1}^{n} \left(\frac{\{D_i \times [T_i] \times 60\}}{[A] \times [Ra]} \right) \tag{1}$$

where:

C – runoff ratio

D_i – stream discharge (m^3/s) at duration of T_i (min)

n – number of the time intervals

Ra – total amount of rainfall (m)

A – area of the catchment to the gauging station which was 9×10^6 m^2

Table 1. The list of data used for the LISEM model

Data	Source
Hydraulic conductivity, *Ks* (mm/h)	field work, some measurements were available from previous research (Hosein 2010)
Soil depth (mm)	field work
Porosity (%)	laboratory measurement
Soil field capacity moisture (in %) as the initial soil moisture	laboratory measurement
Soil bulk density (g/cm^3)	laboratory measurement
Soil texture	field work
Fraction of soil covered by vegetation (%)	field work
Plant height (m)	field work
Hourly rainfall data of Faucon	available in mountain risks project dataset
Faucon stream temporal discharge (m^3/s)	available in mountain risks project dataset
InSAR DTM (15 m resolution)	available in mountain risks project dataset
Land cover map	available in mountain risks project dataset
Roads map	available in mountain risks project dataset
Lithologic map	available in mountain risks project dataset
Geomorphologic map	available in mountain risks project dataset

The runoff ratio was 1.1, which indicates that the stream discharge variations were not caused only by the received rainfall. This could be related to errors in precipitation measurements and unquantified spatial variation in rainfall throughout the watershed. In addition, the base flow of the stream comes from groundwater (Remaitre & Malet 2005) that may originate from other catchments which receive different amounts of rainfall. Since there were no data available for neighbouring catchments and spatial variation in rainfall, model calibration and validation was not possible.

Preparation of morphometric parameters and other environmental maps

The land cover and lithologic maps were available as shape files, projected in Lambert zone III. The map projection system was transformed to UTM (WGS84 zone 32N), re-sampled to a 15 m grid, and then the maps were converted to Raster and ASCII in ArcGIS. The Raster InSAR DTM with 15 m resolution was also transformed to UTM (WGS84 zone 32N) in ArcGIS, then imported to SAGA GIS software (Cimmery 2010). Upon fill-sink operation by the Planchon/Darboux method, the morphometric parameters of LS factor, slope, aspect, wetness index, overland flow distance to channel network, plan-profile curvature and convergence were derived.

Statistical modelling approach

A linear regression approach was run in the R software (Rossiter 2010) so as to analyse the relation between soil depth and the environmental and morphometric parameters. Upon finding the best explanatory variables for the soil depth, the additive and interaction models were investigated using the forward stepwise method (Rossiter 2010).

Kriging of soil depth

The local autocorrelation of soil depth data and residuals of the soil depth model (refer to 2.5.) were determined by variograms and then the ordinary (OK) and regression kriging (RK) was applied. By doing the cross-validation of the kriged maps, the mean error (ME) and root mean squared error (RMSE) were calculated as indices of the prediction accuracy. Finally, the created maps were exported to PCRaster. The conditional simulation of the soil depth was also carried out. The maximum number of nearest observations which would be used for the simulation (n_{max}) and the number of simulations (n_{sim}) were set at 64 (equal to the number of sampling points) and 30, respectively. The number of simulations was selected randomly so as to have sufficient simulated realizations for further analysis.

Preparation of LISEM input maps and the run of model

The LISEM is a physically based model which can simulate erosion, runoff and sediment transport after each rainfall event (Jetten 2002). The model is raster-based and uses PCRaster as the GIS environment (Jetten 2002). Hence, all the produced maps were exported to the PCRaster where the Local Drain Direction (LDD) and other catchment characteristics were derived from the DTM (Jetten 2002).

Three rainfall scenarios were designed based on past events. According to the available rainfall records of 2010, the maximum rainfall intensity of 12 mm/h was used for 2 durations of 60 min and

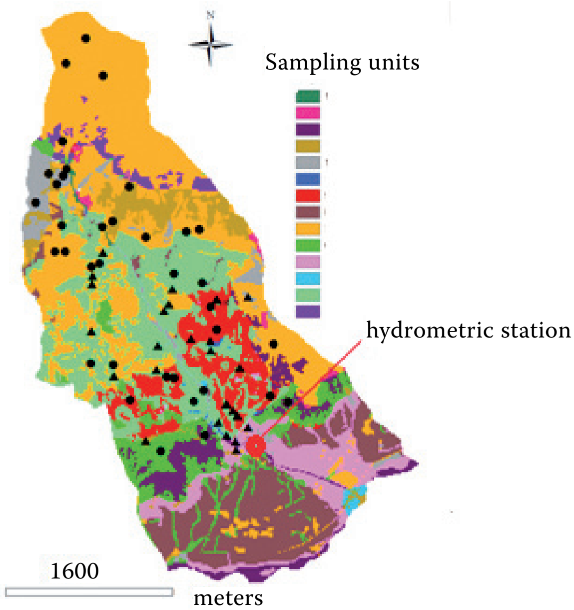

Figure 2. The sampling points; available data locations represent the data acquired by a previous study (Hosein 2010)

Table 2. The validity of soil depth linear models

Variables	Soil depth	
	adjusted R^2	model validity
Land cover	0.44**	valid
Lithology	0.08*	invalid
Slope	0.07*	invalid
Aspect	0.005	invalid
Profile curvature	–0.01	invalid
Plan curvature	–0.01	invalid
Convergence	–0.01	invalid
Wetness index	–0.003	invalid
Overland flow distance to channel network	0.05*	invalid
Elevation	0.03*	invalid
LS	–0.01	invalid

*significant at P = 0.05; **significant at P = 0.01

4 h. Based on Remaitre & Malet (2005), the area has experienced 30 mm/h rainfalls; therefore the latter intensity for duration of 60 min was also introduced as the third scenario. The Green-Ampt and LISEM original interception storage equations were selected in the model run file. The time step of the simulation was selected as 10 s because the cell size of all the maps was 15 m. According to the Courant condition for accuracy and stability, the time step must be smaller than the cell size when using the kinematic wave equation (Hessel 2005).

RESULTS AND DISCUSSION

Statistical analysis on data

According to the statistical analysis of the soil depth dataset, the skewness and kurtosis values were 0.16 and –0.03, respectively, which indicates the lack of normal distribution. The reason could be related to a small number of samples and the applied sampling method. The soil data are not from a random sample but from a purposive one. The soil depth coefficient of variation (CV) was 58%, which indicates low variability of this parameter. In Table 2, the goodness-of-fit of linear models is shown by adjusted R^2. The linear model validity is based on diagnostic plots of the models. Note that the R program enters categorical variables, i.e. Land cover and Lithology, in the regression analysis by the contrasting coding systems (Bruin 2006).

Variables which had a significant relation with soil depth did not have any good diagnostic plots to show the model validity. Only the land cover class was the best explanatory variable for the soil depth (adjusted R^2 =0.44), and resultant linear model parameters were very significant. This could be relevant to the land cover/land use influence on soil protection and erosion. Upon the stepwise forward modelling, adding the terrain parameter of the overland flow distance to channel network raises the soil depth model fit slightly (adjusted R^2 = 0.46). This model had the highest correlation coefficient. That is, just under half of the soil depth variance is explained by land cover class and overland flow distance to channel network. Diagnostic plots of the model were

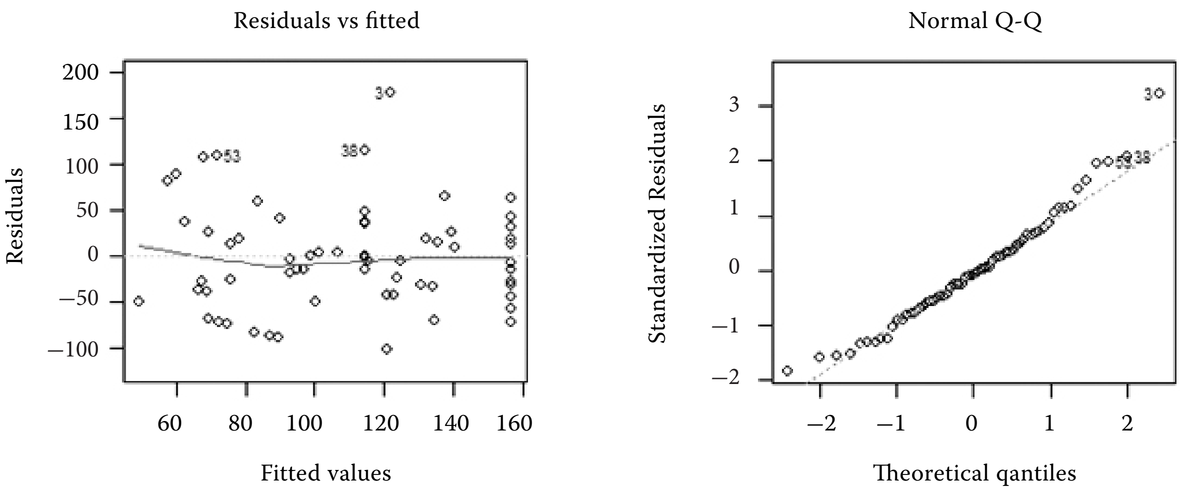

Figure 3. The diagnostic plots of soil depth modelled by land cover and overland flow distance to channel network

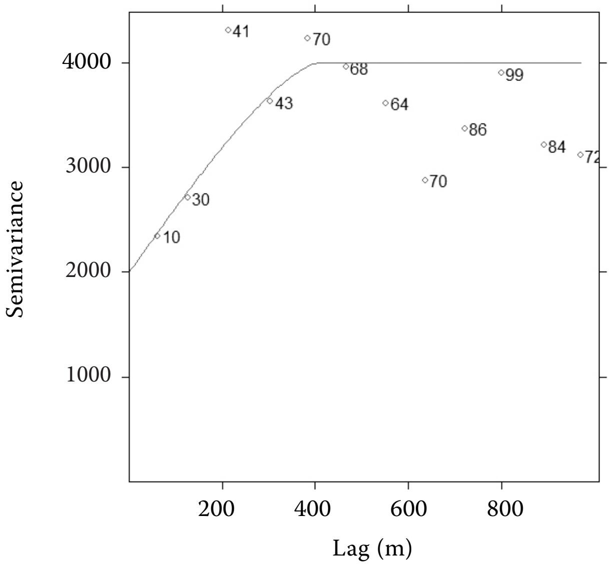

Figure 4. The empirical variogram for soil depth; variogram model = circular, nugget = 2000 mm^2, partial sill = 2000 mm^2, range = 410 m

examined (Figure 3) which looked acceptable. The land cover effect could be discussed with regard to the plant role in soil genesis (Jenny 1941) and soil protection (Foth 1984). Also, topography plays an important role in soil genesis as well as soil erosion and accumulation (Foth 1984; Milevski 2007), so that thicker soils would be expected at lower elevations and on gentler slopes which have concave curvature. However, in different studies, various terrain parameters have been found as the soil depth explanatory variable, for example Herbst & Diekkrüger (2006a, b) reported that the tertiary morphometric parameter of slope elements had the highest correlation with the soil depth while Kuriakose *et al.* (2009) and this study found other terrain parameters.

The results of the present study are compatible with those of Shafique *et al.* (2011), where the additive model of elevation and distance to stream (channel network) was found to best predict the soil depth and the physical reason behind it was attributed to erosion at stream banks.

Ordinary kriging (OK) for soil depth prediction

The empirical variograms of soil depth were plotted in order to understand if there is any spatial structure or not (Figure 4). The best model to fit was a circular variogram.

An ordinary kriging prediction was made for the soil depth. In Figure 5, the results of OK as well as the variance (uncertainty) are shown.

The kriging residuals were obtained by the kriging cross-validation. The residuals were used to calculate the mean error (ME) and root mean squared error (RMSE), which were –0.67 mm and 63.7 mm, respectively. The prediction of RMSE is lower than the average soil depth. Hence, the RMSE was 57% of the average soil depth.

Regression kriging (RK) for soil depth prediction

The autocorrelation of the soil depth model residuals was investigated by a variogram (Figure 6).

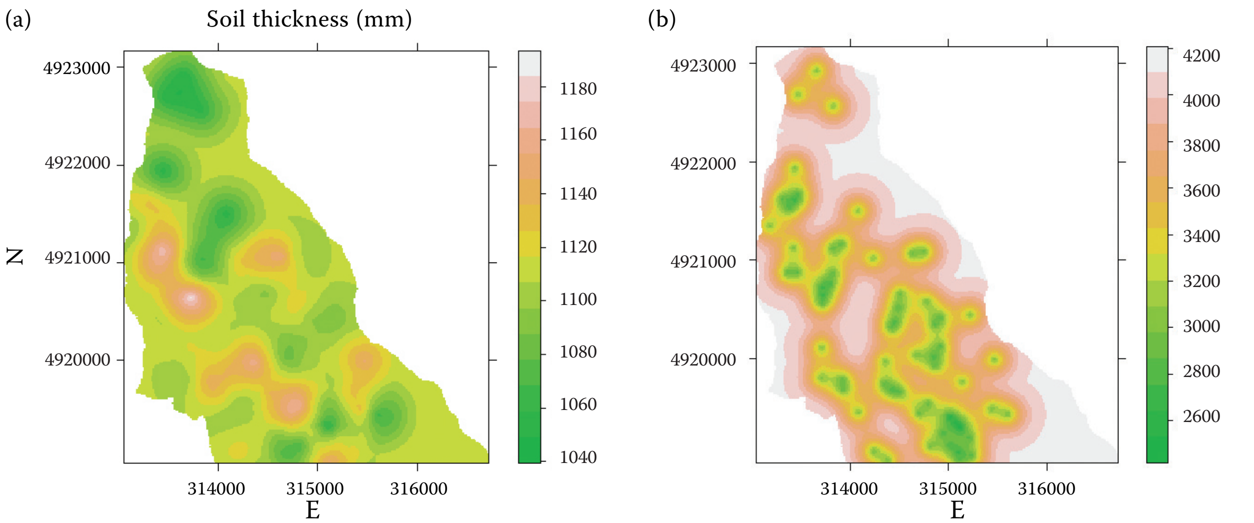

Figure 5. (a) – the map of soil depth made by the ordinary kriging; (b) – the soil depth ordinary kriging variance mm^2

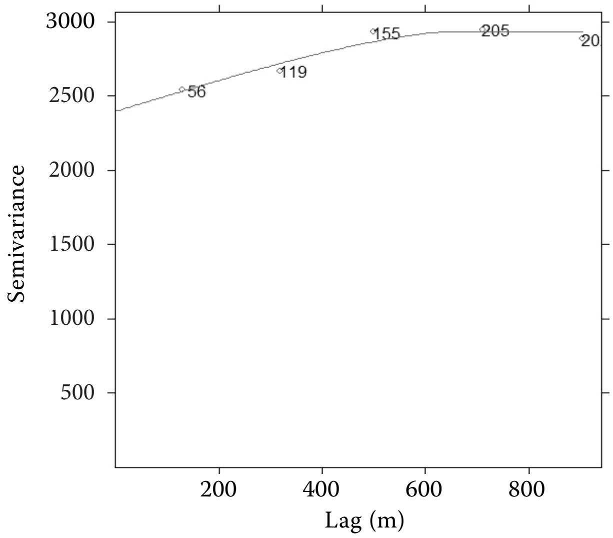

Figure 6. The variogram of soil depth model residuals; Variogram model = circular, partial sill = 537 mm^2, nugget = 2394 mm^2, range = 647 m

The circular model was fitted to the variogram. Because of the residuals spatial structure existence, the next step which was the regression kriging was applied (Figure 7). The map made by the RK shows more variability than the OK map. The RK variance ranges from 0 to 3000 mm^2. The range of the RK variance is lower than that of the OK.

Upon the automatic cross-validation processed by the R, the kriging accuracy was assessed. The ME and RMSE were –2 mm and 60 mm, respectively. The regression kriging RMSE is 54% of the average soil depth, which is slightly lower than that of ordinary kriging. Therefore, the accuracy of the RK is better than that of the OK. A disadvantage of the RK is the production of unreal negative values (Figure 7) which are the interpolation artefacts. Since kriging has a smoothing effect which causes the over- and underestimation of real values (Yamamoto 2005), the conditional simulation can be used to remove the smoothing effect (Webster & Oliver 2007). Based on the cross-validation of the kriging results and RMSE comparisons, the RK produced better results than the OK, thus the RK was implemented for the conditional simulation. Figure 8 shows two realizations of the RK simulation. As Figures 7 and 8 demonstrate, the simulation results are more detailed than the kriged maps.

The LISEM output analysis

Figure 9 shows modelled discharge hydrographs produced by applying two soil depth maps and different rainfall scenarios. The applied maps were named sdok and sdrk which stand for ordinary kriging and regression kriging of soil depth, respectively. According to the Figure, at the beginning of rainfall, the sdrk hydrographs have higher discharge than the sdok, while at the peak the differences are reduced.

The characteristics of produced hydrographs (Table 3) show that the discharge peak of sdrk is higher than that of sdok at scenario (A) where rainfall intensity and duration are the least. As the rainfall duration increases at scenario (B), the peaks of discharge become equal and at scenario (C)

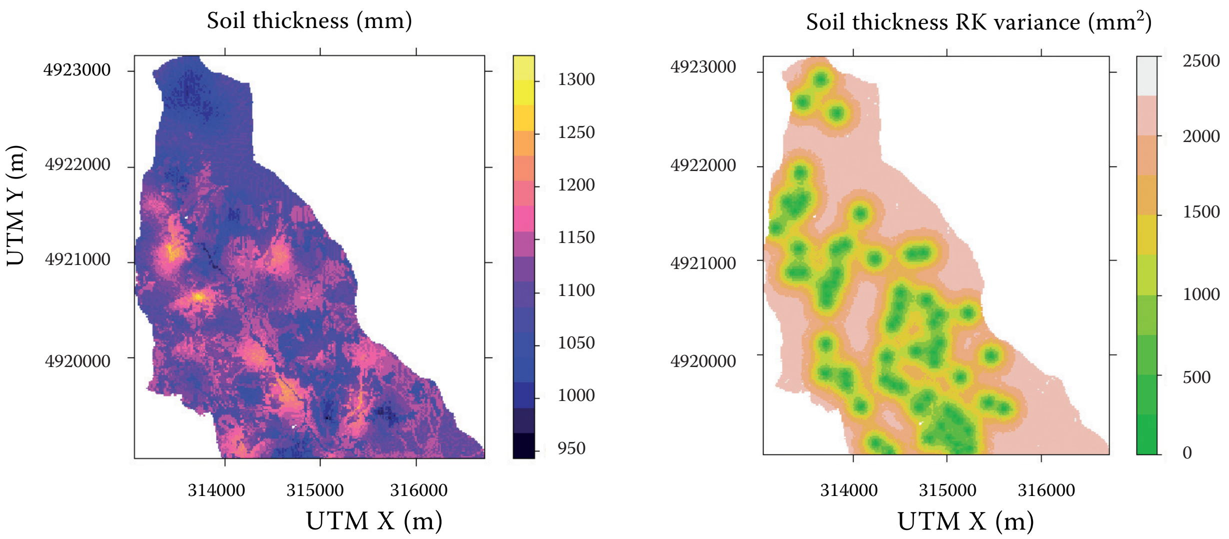

Figure 7. The regression kriging of the soil depth (left) and the kriging variance (right)

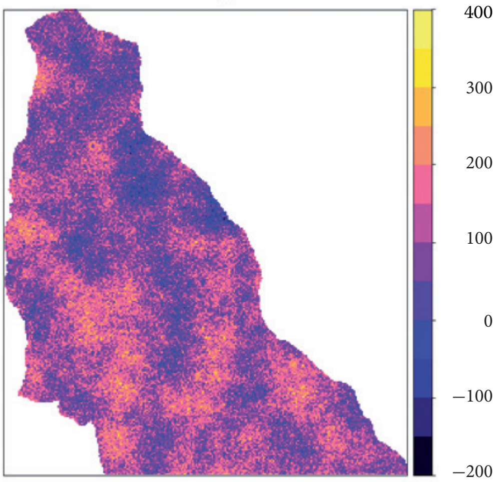

Figure 8. Two simulated realizations of soil depth created by the regression kriging (RK)

where the rainfall intensity is the highest, the discharge peak of the sdok exceeds that of sdrk. At the three rainfall scenarios, the sdrk produced higher total discharge than sdok. As rainfall intensity or duration increases, the total discharge differences decrease. The hydrograph means at each rainfall scenario were compared by the Mann Whitney U (Wilcox) test (Bhattacharjya 2004). The test results revealed that the means of hydrographs, generated at scenario (A), were significantly different at a 95% confidence interval while scenario (B) and (C) did not cause a significant difference in the hydrographs. This could be related to differences in total soil volumes. Figure 10 illustrates the total soil volume of the two soil depth maps. Accordingly, the sdrk has a lower soil volume than the sdok. This means that the sdrk has a lower infiltration capacity for water which increases the saturation overland flow as confirmed by scenario (A). At scenarios (B) and (C), both soils of sdrk and sdok probably reached almost the saturation level at the peak time; hence, the soil depth differences have no effect on water infiltration and the peak discharges are equal or marginally different.

Also, three simulated realizations of the soil depth were selected and analysed in LISEM. The modelled hydrographs are illustrated in Figure 11. The 4th, 10th and 30th realizations of the soil depth simulation are shown as sdrk4, sdrk10 and sdrk30, respectively. The Wilcox test results indicated that the hydrograph means of the scenario (A) were significantly different at a 95% confidence interval while the means of hydrographs at scenarios (B) and (C) were not significantly different.

Based on Figure 11 and Table 3, the sdrk30 produced the highest discharge at the three rainfall scenarios. At scenario (A), where the rainfall intensity was the lowest, the sdrk30 caused the highest peak of discharge. At scenarios (B) and (C), where rainfall duration and intensity increased, respectively, the differences in discharge peaks were reduced. The variations of the hydrograph

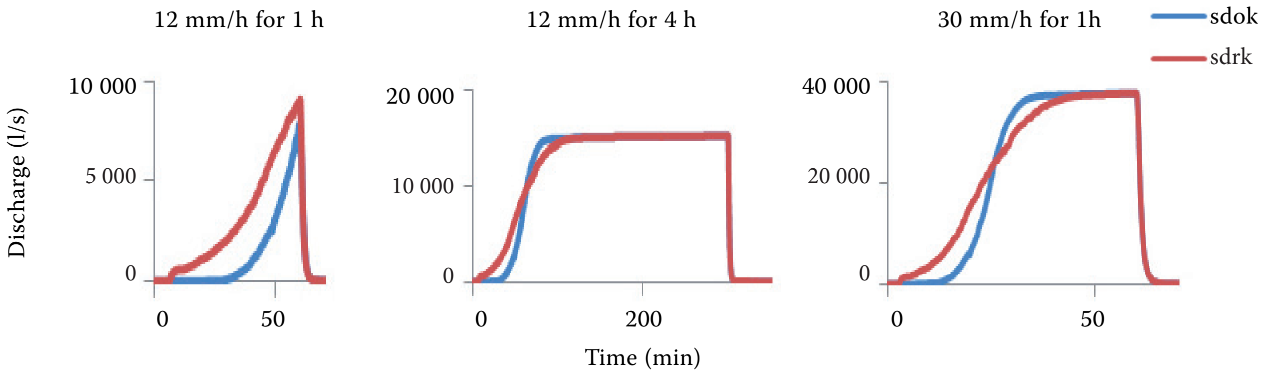

Figure 9. Hydrographs resulting from the application of soil depth ordinary kriging (OK) and regression kriging (RK) at 3 rainfall scenarios

Table 3. Hydrograph characteristics resulting from different interpolation methods at different rainfall scenarios

	sdok	sdrk	sdrk4	sdrk10	sdrk30
(A) 12 mm/h for 1 h					
Peak time (min)	59.6	60	60	60	60
Discharge peak (l/s)	7827	9073	8417	8179	9405
Total discharge (m^3)	5359	11793	13431	13438	16402
(B)12 mm/h for 4 h					
Peak time (min)	299.8	299.8	299.8	299.8	299.8
Discharge peak (l/s)	15 162	15 162	15 162	15 162	15 162
Total discharge (m^3)	219 123	222 643	222 559	221 474	226 143
(C) 30 mm/h for 1 h					
Peak time (min)	59.8	60	60	60	60
Discharge peak (l/s)	37 549	37 533	37 516	37 495	37 510
Total discharge (m^3)	83 018	86 538	86 457	85 374	90 046

sdok – ordinary kriging of soil depth; sdrk – regression kriging of soil depth; sdrk4, sdrk10, sdrk30 – the 4th, 10th and 30th simulated realizations of soil depth

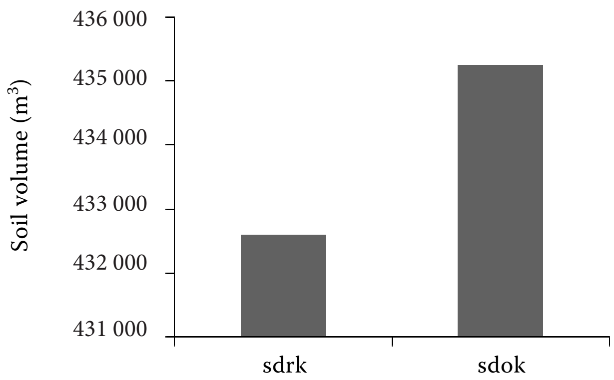

Figure 10. Comparison of the total soil volume of two soil depth maps; sdok = soil depth map produced by the OK; sdrk = soil depth map produced by the RK

characteristics at the three scenarios could be related to differences in the soil volume (Figure 12) and the soil saturation effect as explained earlier (see Figures 9 and 10 for the explanation).

In Table 3, the hydrograph characteristics resulting from RK, OK and RK simulations are brought up together. The peak time is nearly equal at the three rainfall scenarios. At scenario (A), the discharge peaks and total discharges resulting from OK, RK and simulated realizations are substantially different while at scenarios (B) and (C) the differences were largely reduced. The Wilcox test also indicated significant differences in the means of hydrographs produced only at scenario (A). As a whole, various spatial patterns of soil depth have

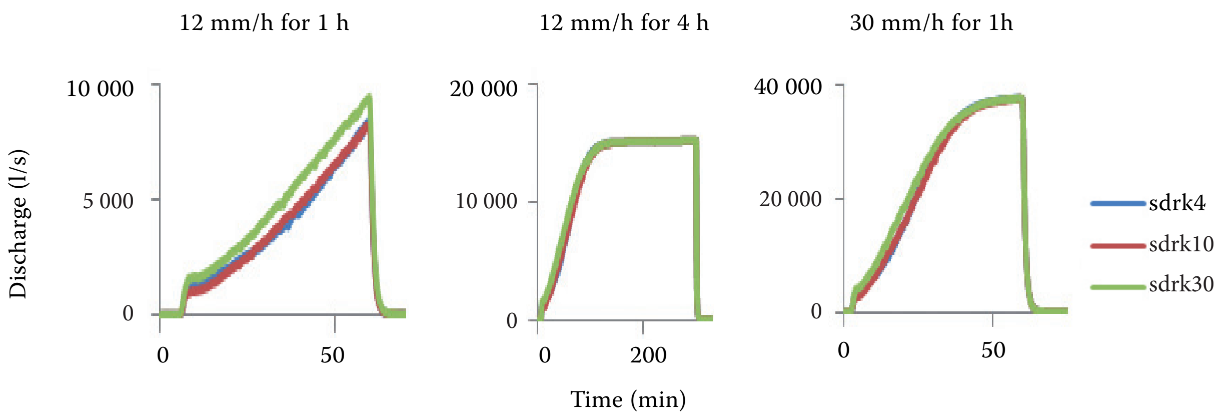

Figure 11. Hydrographs resulting from the application of soil depth regression kriging (RK) simulations

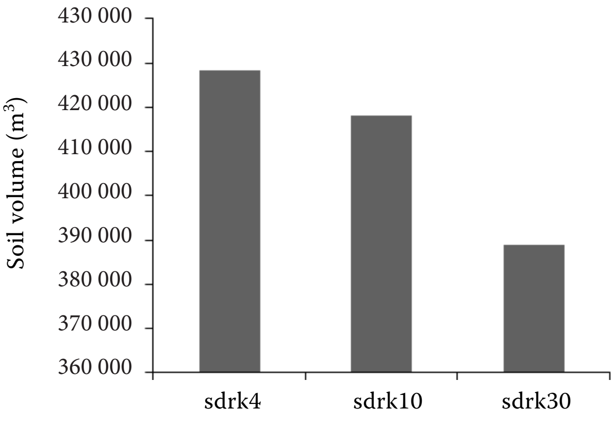

Figure 12. Total soil volumes of the simulated realizations

no significant effect on hydrograph modelling at rainfalls of high intensity and/or long duration.

CONCLUSION

The study was conducted to find out how well the environmental and terrain variables could predict the soil depth as well as to understand the importance of differences in the soil depth variation in relation to hydrograph modelling. Based on the findings, the additive linear model of land cover and terrain parameter of overland flow distance to channel network better predicted the soil depth, though due to the lack of sufficient amounts of sampled data, the validation could not be implemented. This confirms the results of Kuriakose *et al.* (2009) and Shafique *et al.* (2011). In the present study the minor effect of overland flow distance to channel network may be a proxy for soil depth prediction. According to the cross-validation results, the regression kriging of soil depth using the "land cover" and "overland flow distance to channel network" variables provided better results than the ordinary kriging. This finding is compatible with that of Kuriakose *et al.* (2009). The RK prediction was however fairly uncertain (RMSE 60 mm, over a half the median depth 107 mm), and away from sample points the kriging prediction variance and standard deviation were of the same order of magnitude, about 500 mm^2 and 22 mm, respectively. This uncertainty is expected to have a major effect on any model sensitive to soil depth. The reason for the high uncertainty is having few points and poor spatial structure with high nugget effect.

The hydrologic model was sensitive to different spatial variations of the soil depth at rainfall of low intensity and/or short duration. As the intensity or duration of rainfall increases, the hydrograph differences diminish, so that they can become insignificant. This is because at rainfalls of short duration or low intensity the soil may not reach the near saturation level; hence, the shallower soils are saturated faster and produce more runoff than the deeper soils. But at higher intensity or duration of rainfall, all soils may reach the saturation. Therefore, the soil depth variations make no more differences in the runoff generation.

Acknowledgements. The research was financed by the Faculty of Geo-Information Science and Earth Observation of University of Twente. Hereby I acknowledge the great support of Prof. V. Jetten and Dr. D. Rossiter from the University of Twente. I also express great appreciation to Dr. J.P. Malet, Dr. C. van Westen and Dr. D. Alkema, who provided me with the Mountain Risks Project dataset.

References

Bagarello V., Sferlazza S. (2009): Comparing two methods of analysis of single-ring infiltrometer data for a sandy-loam soil. Geoderma, **149**: 415–420.

Bhattacharjya R.K. (2004): Optimal design of unit hydrographs using probability distribution and genetic algorithms. Sadhana, **29**: 499–508.

Bruin J. (2006): Newtest: Command to Compute New Test. UCLA: Academic Technology Services, Statistical Consulting Group. Available at http://www.ats.ucla.edu/stat/stata/ado/analysis/ (accessed September 2011).

Cimmery V. (2010): User Guide for SAGA (version 2.0.5). Vol. 1 and 2. Available at http://www.saga-gis.org/en/about/references.html (accessed January 16, 2011).

De Roo A.P.J. (1996a): The LISEM project: An introduction. Hydrological Processes, **10**: 1021–1025.

Dietrich W.E., Reiss R., Hsu M.-L., Montgomery D.R. (1995): A process-based model for colluvial soil depth and shallow landsliding using digital elevation data. Hydrological Processes, **9**: 383–400.

FAO (2006): Guidelines for Soil Description. 4th Ed. FAO, Rome.

Farrell Z. (2010): Single Ring Falling Head Infiltrometer. Available at http://www.usyd.edu.au/agric/web04/Single%20ring%20final.htm (accessed October 2010).

Florinsky I.V., Eilers R.G. (2002): Prediction of soil properties by digital terrain modelling. Environmental Modelling & Software, **17**: 295–311.

Foth H.D. (1984): Fundamentals of Soil Sciences. 7th Ed. John Wiley and Sons, Inc., New York.

Green W.H., Ampt G.A. (1911): Studies on soil physics. 1. The flow of air and water through soils. Journal of Agricultural Sciences, **4**: 11–24.

Goovaerts P. (2000): Geostatistical approaches for incorporating elevation into the spatial interpolation of rainfall. Journal of Hydrology, **228**: 113–129.

Grayson R., Bloschl G. (eds) (2001): Spatial Patterns in Catchment Hydrology; Observations and Modeling. University Press, Cambridge.

Herbst M., Diekkrüger B. (2006a): Numerical experiments on the sensitivity of runoff generation to the spatial variation of soil hydraulic properties. Journal of Hydrology, **326**: 43–58.

Herbst M., Diekkrüger B. (2006b): Geostatistical co-regionalization of soil hydraulic properties in a micro-scale catchment using terrain attributes. Geoderma, **132**: 206–221.

Hessel R. (2005): Effects of grid cell size and time step length on simulation results of the Limburg soil erosion model (LISEM). Hydrological Processes, **19**: 3037–3049.

Hosein T. (2010): Alluvial Fan Flood Hazard Assessment based on DTM Uncertainty. [MSc Thesis.] ITC, Enschede.

Jenny H. (1941): Factors of Soil Formation, a System of Quantitative Pedology. McGraw-Hill, New York.

Jetten V.G. (2002): LISEM User Manual. Utrecht Center for Environment and Landscape Dynamics, Utrecht University, Utrecht.

Jetten V., Straatsma M., Alkema D. (2010): Spatial Modelling of Natural Hazard Processes, GH Module 8. ESA Department, ITC, Enschede.

Kalivas D.P., Triantakonstantis D.P., Kollias V.J. (2002): Spatial prediction of two soil properties using topographic Information. Global Nest: the International Journal, **4**: 41–49.

Kuriakose S.L., Sanjaya Devotka, Rossiter D.G., Jetten V.G. (2009): Prediction of soil depth using environmental variables in an anthropogenic landscape, a case study in the Western Ghats of Kerala, India. Catena, **79**: 27–38.

Kutilek M., Nielsen D.R. (1994). Soil Hydrology. Catena Verlag Geoecology Publications, Cremlingen-Destedt.

Malet J.-P., Remaitre A., Maquaire O. (2004): Runout modeling and extension of the threatened area associated with muddy debris flows. Géomorphologie: Relief, Processus, Environment, **10**: 195–209.

McBratney A.B., Mendonça Santos M.L. (2003): On digital soil mapping. Geoderma, **117**: 3–52.

McKenzie N.J., Ryan P.J. (1999): Spatial prediction of soil properties using environmental correlation. Geoderma, **89**: 67–94.

Merz B., Bárdossy A. (1998): Effects of spatial variability on the rainfall runoff process in a small loess catchment. Journal of Hydrology, **212**–**213**: 304–317.

Milevski I. (2007): Morphometric elements of terrain morphology in the Republic of Macedonia and their influence on soil erosion. In: Int. Conf. Erosion 2007. Belgrade.

Minasny B., McBratney A.B. (1999): A rudimentary mechanistic model for soil production and landscape development. Geoderma, **90**: 3–21.

Mountain Risks (2010): The Faucon watershed: the 2003 debris-flow even (part 1). Available at_http://www.unicaen.fr/mountainrisks/spip/IMG/pdf/13_Faucon_pit_stop_1.pdf (accessed August 17, 2010).

Mwendera E.J., Feyen J. (1992): Estimation of depression storage and Manning's resistance coefficient from random roughness measurements. Geoderma, **52**: 235–250.

Neitsch S.L., Arnold J.G., Kiniry J.R., Williams J.R., King K.W. (2002): Soil and Water Assessment Tool. Theoretical Documentation. TWRI Report, Texas Water Resources Institute, Texas.

Odeh I.O.A., McBratney A.B., Chittleborough D.J. (1995): Further results on prediction of soil properties from terrain attributes: heterotopic cokriging and regression-kriging. Geoderma, **67**: 215–226.

OMIV-EOST (2010): Barcelonnette area, debris flows at Faucon. Services des Observatoires des instabilites de Versants. Available at_http://eost.u-strasbg.fr/omiv/barcelo_area_faucon.html (accessed August 17, 2010).

Penížek V., Borůvka L. (2006): Soil depth prediction supproted by primary terrain attributes: a comparison of methods. Plant, Soil and Environment, **52**: 424–430.

Prachansri S. (2007): Analysis of soil and land cover parameters for flood hazard assessment: a case study of the Nam Chun watershed, Phetchabun, Thailand. [MSc Thesis.] ITC, Enschede.

Remaitre A., Malet J.P. (2005): Morphology and Sedimentology of a complex Debris Flow in a clay-shale basin. Earth surface processes and landforms. The Journal of British Geomorphological Research Group, **30**: 339–348.

Renard K.G., Foster G.R., Weesies G.A., McCool D.K., Yoder D.D. (2000): Predicting Soil Erosion by Water: A Guide to Conservation Planning with the Revised Universal Soil Loss Equation (RUSLE). The U.S. Department of Agriculture (USDA), Washington D.C.

Rossiter D.G. (2010): Tutorial: Using the R Environment for Statistical Computing. An Example with the Mercel & Hall Wheat Yield Dataset. Faculty of

Geo-Information Science & Earth Observation (ITC), University of Twente, Enschede.
Shafique M., van der Meijde M., Rossiter D.G. (2011): Geophysical and remote sensing-based approach to model regolith thickness in a data-sparse environment. Catena, **87**: 11–19.
Singh V.P. (1997): Effect of spatial and temporal variability in rainfall and watershed characteristics on stream flow hydrology. Hydrological Processes, **11**: 1649–1669.
USDA (2010): Determining Soil Texture by Feel Method Handout. Available at http://www.mt.nrcs.usda.gov/about/lessons/Lessons_Soil/feelmethod.html (accessed October 17, 2010).
Webster R., Oliver M.A. (2007): Geostatistics for Environmental Scientists. 2nd Ed. John Wiley and Sons, Ltd, Chichester.
Yamamoto J. (2005): Correcting the smoothing effect of ordinary kriging estimates. Mathematical Geology, **37**: 69–94.
Ziadat F.M. (2010): Prediction of soil depth from digital terrain data by integrating statistical and visual approaches. Pedosphere, **20**: 361–367.

Received for publication May 17, 2011
Accepted after corrections April 2, 2012

Corresponding author:

Pooyan Rahimy, MS.c., University of Guelph, School of Environmental Sciences, Guelph, ON, Canada
e-mail: sama.pooyan@gmail.com